Intratracheal Transplantation of Trophoblast Stem Cells Attenuates Acute Lung Injury in Mice

Junwen Han
Brigham and Women's Hospital
Gu Li
Brigham and Women's Hospital
Minmin Hou
Brigham and Women's Hospital
Min-Young Kwon
Brigham and Women's Hospital
Kevin Xiong
Brigham and Women's Hospital
Xiaoliang Liang
Balyor College of Medicine
Elizabeth Taglauer
Boston Children's Hospital
Yuanyuan Shi
Beijing University of Chinese Medicine
S Alex Mitsialis
Boston Children s Hospital
Stella Kourembanas
Boston Children's Hospital
Souheil El-Chemaly
Brigham and Women's Hospital
Ivan O Rosas
Baylor College of Medicine
Mark A Perrella
Brigham and Women's Hospital
Xiaoli Liu (xlliu@rics.bwh.harvard.edu)
Brigham and Women's Hospital https://orcid.org/0000-0003-2904-4413

Research

Keywords: Trophoblast stem cells, acute lung injury, inflammation, alveolar 19 epithelial cells, engraftment

Posted Date: August 28th, 2020

DOI: https://doi.org/10.21203/rs.3.rs-63519/v1

Version of Record: A version of this preprint was published at Stem Cell Research & Therapy on August 30th, 2021. See the published version at https://doi.org/10.1186/s13287-021-02550-z.

Intratracheal Transplantation of Trophoblast Stem Cells Attenuates Acute Lung Injury in Mice

Junwen Han M.D.[1,4], Gu Li, M.D.[5], Minmin Hou M.D., Ph.D.[1], Min-Young Kwon, Ph.D.[1], Kevin Xiong[1], Xiaoliang Liang, Ph.D.[1,2], Elizabeth Taglauer, M.D., Ph.D.[3], Yuanyuan Shi, Ph.D.[4], S Alex Mitsialis Ph.D[3], Stella Kourembanas M.D.[3], Souheil El-Chemaly, M.D.[1], Ivan O Rosas, M.D.[1,2], Mark A Perrella, M.D.[1,5], and Xiaoli Liu, M.D., Ph.D*[1,5]

[1]Department of Medicine, Division of Pulmonary and Critical Care Medicine, Brigham and Women's Hospital, Boston, MA, 02115, USA; [2]Department of Medicine, Division of Pulmonary, Critical Care and Sleep Medicine, Baylor College of Medicine, TX, 77024, USA; [3]Department of Pediatrics, Division of Newborn Medicine, Boston Children's Hospital, Boston, MA, USA 02115; [4]School of Life Sciences, Beijing University of Chinese Medicine, Beijing 100029, China. [5]Department of Pediatric Newborn Medicine, Brigham and Women's Hospital, Boston, MA, 02115, USA

*Address correspondence to: Xiaoli Liu, M.D., Ph.D., Division of Pulmonary and Critical Care Medicine, Brigham and Women's Hospital, 75 Francis Street, Boston, MA 02115, USA. Tel: (617)732-6910; Fax: (617)264-6365; E-mail: xlliu@rics.bwh.harvard.edu

Abstract

Background

Acute lung injury (ALI) is a common lung disorder that affects millions of people every year. The infiltration of inflammatory cells into the lungs and death of the alveolar epithelial cells are key factors to trigger a pathological cascade. Trophoblast stem cells (TSCs) have been shown to possess immune privilege, immunomodulation, and the potential of self-renewal and multipotency with differentiation into three germ layers. We hypothesized that intratracheal transplantation of TSCs may alleviate ALI.

Methods

ALI was induced by intratracheal delivery of Bleomycin (BLM) in mice. At day 3 after exposure to BLM, pre-labeled TSCs or Fibroblasts (FBs) were intratracheally administered into the lungs. At day 7 after exposure to BLM, histological analyses of the lungs were performed for inflammatory infiltrates, cell apoptosis, and engraftment of TSCs. Pro-inflammatory cytokines/chemokines of lung tissue and in bronchoalveolar lavage fluid (BALF) were also assessed by quantitative real-time polymerase chain reaction and enzyme-linked immunosorbent assays, respectively. Flow cytometry was utilized to assess engraftment of TSCs and cell apoptosis.

Results

Histological analyses of the lungs displayed a reduction in cellularity and less thickening of the alveolar walls in ALI mice that received TSCs compared with

ALI mice receiving PBS or FBs. TSCs decreased infiltration of neutrophils and macrophages, and the expression of interleukin 6 (IL-6), monocyte chemoattractant protein-1 (MCP-1) and keratinocyte-derived chemokine in the injured lungs. The levels of IL-6 and MCP-1 in BALF were decreased in ALI mice receiving TSCs, compared with ALI mice that received PBS or FBs. Terminal deoxynucleotidyl transferase dUTP nick end labeling confirmed that TSCs significantly reduced BLM-induced apoptosis of lung tissue *in vivo and* epithelial cells *in vitro*. Transplanted TSCs integrated into the alveolar walls and expressed aquaporin 5 and prosurfactant protein C, markers for alveolar epithelial type I and II cells, respectively.

Conclusion

Intratracheal transplantation of TSCs into the lungs of mice after acute exposure to BLM reduced pulmonary inflammation and cell death. Furthermore, TSCs engrafted into the alveolar walls to form alveolar epithelial type I and II cells. These data support the use of TSCs for the treatment of ALI.

Keywords: Trophoblast stem cells, acute lung injury, inflammation, alveolar epithelial cells, engraftment

Background

Acute lung injury (ALI) is a common and devastating respiratory disorder, with

an annual incidence of 86.2 per 100,000 people, and the hospital mortality rate for all patients is close to 40%(1, 2). There are 190,600 acute cases in the United States each year, which is associated with 74,500 deaths and 3.6 million hospital days (1, 2). In patients who survive ALI, their long-term quality of life is severely affected. Thus, there is an unmet need for better treatment options for patients with ALI (1, 2). The causes of ALI are diverse, lung infections of various pathogens, sepsis, harmful chemicals, and even antineoplastic therapies. The pathogenesis is still not completely clear, but the histopathological features of ALI in patients and animal models indicate that inflammatory cell infiltration in the lungs and alveolar-capillary barrier damage resulting from the death of the alveolar epithelial type I/II and endothelial cells. Damaged alveolar epithelial type II cells impair pulmonary surfactant secretion and alveolar clearance, resulting in lung edema, which eventually causes impaired gas exchange, hypoxemia, and the development of acute respiratory distress syndrome (ARDS)(1, 2).

Stem cells have been demonstrated to possess properties that promote reparation and regeneration, and to mediate inflammation and protect cells from death via paracrine effects (3, 4). Transplantation of stem cells has been applied to treat ALI in humans and various animal models(5-13). Mesenchymal stem/stromal cells (MSCs) are the most investigated cells and have been demonstrated to reduce the inflammatory response in experimental ALI(4, 6), and shown to be safe when administered to patients

with ARDS(9, 12, 13). The current view is that the therapeutic properties of MSCs are derived from paracrine actions, while MSC engraftment is limited(4, 14, 15). Experimental observations of endothelial progenitor cells(11), bone marrow-derived mononuclear cells(5), embryonic stem cells (ESCs) and induced pluripotent stem cells (iPSCs) in the treatment of ALI have also been investigated(7, 8, 10). A population of alveolar epithelial progenitor cells is considered a facultative progenitor cell within the distal lung, and has been shown to produce lung regeneration in ALI(16).

The placenta is an organ typically discarded after birth, and contains a variety of stem cells(17-21) that can be easily obtained and banked. Placenta-derived stem cells are thought to be young cells, with plasticity between that of ESCs and adult stem cells(18, 22, 23). Most of the placenta-derived stem cells used for therapeutic studies of experimental ALI are MSCs(24), and amnion epithelial cells(25, 26). MSCs appear to play a role in protection and immunomodulation via paracrine actions(27), while amnion epithelial cells show evidence of prevention and repair of experimental lung injury(25, 26). In contrast to these prior investigations, the present study focuses on the use of trophoblast stem cells (TSCs). TSCs are a unique cell population of stem cells and have been shown to differentiate into all other types of trophoblast cells in the placenta(28), as well as three germ layers of the fetus(29). Interestingly, when blastocysts or cones (the origin of TSCs) were introduced directly into the lung, trophoblast cells grew in 30-50% of mice(30). Furthermore, TSC-

derived trophoblast cells have been demonstrated to play a key role in interacting with maternal leukocytes to maintain immune homeostasis during pregnancy via production of hormones, cytokines, and other factors(31-33). The unique immune privilege of TSCs protects the fetus from maternal targeting by immune cells, such as T lymphocytes and natural killer cells(18, 22). To our knowledge, no investigation of TSCs in experimental ALI has been reported.

In a recent article, using CD117 as a cell surface marker of stem cells, we demonstrated positive cells located in the labyrinth zone and chorionic basal plate of the E18.5 mouse placenta(29). These $CD117^{+}$ trophoblast cells, isolated from the near term placenta (E18.5), have the stem cell properties of clonogenicity, self-renewal, and multipotency of differentiation into three germ layers, including alveolar epithelium type I and II cells(29). In this study, we will intratracheally delivery Bleomycin (BLM) to induce ALI and then transplant TSCs into the lungs of mice. BLM, a chemotherapeutic drug, causes acute lung inflammation and alveolar epithelial cell death in the first week after exposure(34, 35). The effect of TSCs in ALI was assessed for tissue inflammation, alveolar cell injury/death, and engraftment of TSCs during this 7 day period after BLM exposure. In this study, we demonstrate for the first time that TSCs play an important role in mediating tissue inflammation, preventing lung injury, and engrafting and differentiating into alveolar epithelial cells in this experimental model of ALI in mice.

Materials and Methods

ALI induced by intratracheal delivery of BLM into mice.

Male 8-10 weeks C57BL/6 black mice were randomly divided into 2 groups. Intratracheal delivery of PBS (sham) or BLM (ALI) was performed as previously described(8, 36). Briefly, mice were anesthetized with Ketamine (10mg/kg) and Xylazine (100mg/kg), and the skin of the neck was sterilized with 75% ethanol. The mice were secured on a surgical board and the skin was carefully cut to expose the trachea. The surgical board was then adjusted to an incline of 75°, and a 30G needle was inserted into the trachea to generate a hole. Then using a blunt end 30G needle, 100 μl of PBS or BLM (Bleomycin Sulfate, Cayman Chemical, Cat#13877) diluted in 100 μl PBS at a concentration of 0.75mg/kg was intratracheally injected into the lungs of mice (day 1), and the subcutaneous membrane and skin were subsequently sutured. Mice were then allowed to recover from the procedure and anesthesia. The use of mice and the studies performed were carried out in accordance with the Public Health Service policy on the humane care and use of laboratory animals, and the protocol was approved by the Institutional Animal Care and Use Committee of Brigham and Women's Hospital.

Intratracheal delivery of PBS/cells into mice.

At day 3 after exposure to PBS or BLM, TSCs and fibroblasts (FBs) were pre-labeled with PKH67 green fluorescent dye (for details see “Labeling TSCs and FBs”). Sham mice were injected with PBS only (sham+PBS). ALI mice were divided into three groups (6~8 mice per group), receiving intratracheal administration of 100μl PBS (ALI+PBS), FBs (ALI+FB, $0.5X10^6$ cells in 100μl PBS), or TSCs (ALI+TSCs, $0.5X10^6$ cells in 100μl PBS). The procedure was the same as the intratracheal delivery of BLM. The mice were harvested at day 7 after BLM exposure.

Isolation and culture of $CD117^+$ TSCs.

TSCs were harvested as previously described (29). Briefly, placentas were collected at embryonic day (E) 18.5 from pregnancies of wild-type C57BL/6 mice, and also from heme oxygenase-1 (HO-1) null mice, as previously described(37). The maternal portion was trimmed off (~1mm), and the remaining placental tissue was chopped into small pieces and dissociated in an enzyme buffer containing collagenase I (1mg/ml) and collagenase II (2.5 mg/ml, Worthington Biochemical) in PBS for 30~45 minutes. After filtering through a 100μl strainer, cells were cultured in DMEM/F12 (Lonza) supplemented with 20% fetal bovine serum (FBS, GE Healthcare), 100mM nonessential amino acids (Cellgro), 55mM beta-mercaptoethanol (Gibco), 1mM sodium pyruvate (Cellgro), 10ng/ml LIF (Millipore), 20ng/ml murine basic fibroblast growth factor (PeproTech), and 1% penicillin/streptomycin/L-

glutamine (Corning). Culture medium was changed every other day. TSCs were isolated using anti-mouse CD117 MicroBeads (Miltenyi Biotec, Cat. 130-091-224)(29). The wild-type clonal $CD117^{+}$TSCs were obtained from a limiting dilution culture (see details in “Limiting dilution and clone formation in vitro”), and then expanded. TSCs were further characterized using immunofluorescence staining or flow cytometry.

Isolation of lung FBs.

FBs were harvested as previously described (38). Briefly, the lungs were harvested from wild-type C57/BL6 mice, and FBs isolated by lineage negative/Sca1-depleted beads. The cells were plated in medium and expanded prior to immunophenotyping and use.

TSCs and FBs labeled with the green fluorescent dye PKH67.

TSCs or FBs were labeled with the green fluorescent dye PKH67 (SIGMA, Cat. MINI67-1KT), which incorporates into the membrane of cells and is equally distributed to daughter cells when they divide. The procedure was followed using the standard protocol of Millipore-Sigma.

Bronchoalveolar lavage fluid (BALF) of mice.

Mice were sacrificed by injecting Ketamine and Xylazine at 7 days after BLM exposure. The trachea was exposed and cannulated with a blunted 23G

needle and ligature, as previously described(31, 34). 500μl PBS was slowly administered into the lungs of mice, and then the BALF was withdrawn and repeated once, a total of 600 to 800 μl of BALF was collected for cell counts, cytospins, and ELISA(34). Briefly, the BALF samples were centrifuged at 4000rpm for 5 min at 4 °C, and the supernatant was stored in -80 °C for ELISA. The cells were resuspended in 500 μl PBS for cell counting or flow cytometry analysis.

Cell differential of neutrophils and macrophages in BALF.

The cells from BALF were resuspended in 500 μl PBS, and 100 μl cell suspensions were cytospun, at 350 rpm for 3min, onto a slide. The slides then were stained with Hema 3 Manual Staining System and Stat Pack (Fisher Scientific, Catalog No.23-123869). The protocol followed the manufacturer's instructions. After staining, the percentages of BAL neutrophils and macrophages were obtained by counting 300 leukocytes on randomly selected portions of the slide by light microscopy.

Enzyme-linked immunosorbent assay (ELISA).

The concentration of interleukin 6 (IL-6) and monocyte chemoattractant protein-1 (MCP-1) in the BALF of mice was measured using Mouse IL-6 Quantikine ELISA Kit (R&D systems, Cat#: M6000B), and Mouse CCL2/JE/MCP-1 Quantikine ELISA Kit (R&D systems, Cat#: MJE00B),

following the manufacturer's instructions. The concentration of each protein in the BALF samples was measured by comparing the optical density (OD) using a Microplate Reader (Bio-Tek). Standard curves were calculated for each ELISA kit.

Limiting dilution and clone formation of TSCs.

100 $CD117^+$ TSCs were plated in 100 mm diameter dish (the density, ≈1 cell/60 mm^2) to obtain multicellular clones derived from a single founder cell(29). Growth medium was changed every 3 days and the clones formed over 2–3 weeks. The clones were then imaged by phase contrast microscopy and fluorescent microscopy for CD117 immunostaining. The clones were also harvested using cloning cylinders and then expanded in culture for all experiments.

Differentiation of TSCs into airway epithelial cell.

$CD117^+$ TSCs were seeded on the apical side of a clear 12-transwell plate (ThermoFisher, Cat#3460) at a density of 65,000 cells/well and cultured in growth medium for 2 days(29). Then cells were exposed to 2% FBS DMEM/F12 differentiation medium supplied with 0.005mg/ml insulin (Sigma, Cat# 10516), 0.01mg/ml Tranferrin (Sigma, Cat# T8158), 30nM Sodium selenite (Sigma, Cat# S5261), 10nM Hydrocortisone (Sigma, Cat#H6909), 10nM Beta-estradiol (Sigma, Cat# E2758), 10nM HEPES (FisherBiotech, Cat#

H0887), 2mM L-glutamine (ATTC, Cat# 30-2214) and 50ng/ml EGF (PeproTech, Cat# AF-100-15) for another 5~6 days. Once the cells reached complete confluence, the air-liquid interface was established by adding the differentiation medium to basal side and allowing the apical side to be exposed to air, for an additional 11~12 days. Cells were harvested for immunofluorescence staining and quantitative real-time PCR (qRT-PCR).

Flow cytometry analysis.

Two lobes of the right lung were digested using collagenase and then filtered through a 40um filter, as previously described(29). After generating the single cell suspensions, the cells were fixed for 30min at room temperature (RT) and then permeabilized for 30 min at RT. Cells were blocked with 10% donkey serum at RT for 30min and incubated with primary antibodies aquaporin 5 (AQP5; EMD Millipore, Cat. AB15858, 1:100) and prosurfactant protein C (SPC; Abcam, Cat. ab40879, 1:100) at 4ºC for 30 min in darkness. The secondary antibody conjugated with fluorescence was diluted in the permeable buffer in 1:100 for 30min on ice. The cells were then assessed using BD FACS Canto II and the data was analyzed using FlowJo software (TreeStar).

Immunohistochemistry staining.

The mouse lungs were harvested at day 7 after BLM exposure and then fixed in 10% formalin overnight. The lungs were then dehydrated, embedded in paraffin and cut into a 5 μm in thickness, as previously described(29). To improve antigen recognition, the sections were microwaved in 10 mM Citrate Buffer (pH6.0) for 10~12 minutes. The tissue was blocked in 10% normal donkey serum for 30 min at RT and then incubated in the primary antibody AQP5 (1:100) or SPC (1:100), at 4°C overnight. Second antibodies were conjugated with fluorescence, then were incubated with samples at 37 °C for 1 h. Nuclei were stained with 4′,6-diamidino-2-phenylindole (DAPI; 1:1000 in PBS) at 37 °C for 10 min. Images were analyzed using fluorescence microscopy and confocal microscopy system (Olympus). Staining of the lungs was also performed for Hematoxylin and Eosin, and CD45 (BD Biosciences, Cat# 553078) immunostaining using DAB, following the manufacturer's protocol.

Immunocytochemistry staining.

Immunocytochemistry was performed as previously described(29). Cells were fixed with 4% paraformaldehyde at RT for 10 min, and permeabilized with 0.2% Triton X-100 at RT for 10 min. Next, cells were blocked in 10% donkey serum at RT for 30 min and then incubated in the primary antibodies AQP5 (1:100) and SPC (1:100) at 4 °C overnight. The second antibodies conjugated with fluorescence were incubated with the samples at 37 °C for 1 h and nuclei were

stained with DAPI (1:1000) in PBS) at 37 °C for 10 min. Images were analyzed using fluorescence microscopy and confocal microscopy system (Olympus).

Terminal deoxynucleotidyl transferase dUTP nick end labeling (TUNEL).

Lung sections were stained to assess apoptosis as descripted previously(39). Briefly, the sliders were rehydrated in gradient concentration of ethanol and fixed with 4% formaldehyde for 15min at RT. After treating with 20ug/ml proteinase K for 10min at RT, tissue was stained with the mixed buffer, including equilibration buffer 45ul, nucleotide mix with fluorescein isothiocyanate (FITC) 5ul and TdT enzyme 1ul per each slide, for 1h at 37°C, following a nuclear staining with the DAPI (1:1000).

qRT-PCR.

Total RNA was extracted from cells or tissues using Trizol reagent (Invitrogen). cDNA was made by reverse-transcription using the SuperScript III First-Strand Synthesis System (Invitrogen). qRT-PCR analyses were performed using the Syber Green kit (Bio-Rad), and data were analyzed by the ΔC_T threshold cycle method. AQP5: 5′-CTCCCCAGCCTTATCCATTG-3′, 5′-CCAGAAGACCCAGTGAGAGG-3′;

SPC: 5′-CAAACGCCTTCTCATCGTGGTTGT-3′, 5′-TTTCTGAGTTTCCGGTGCTCCGAT-3′;

IL-6: 5'-CAAAGCCAGAGTCCTTCAGAG-3', 5'=GTCCTTAGCCACTCCTTC-3'; MCP-1: 5'-GCTCTCCAGCCTACTCATTG-3', 5'GTCCCTGTCATGCTTCTGG-3'; Keratinocyte-derived chemokine (KC): 5'-CAGACGGTGCCATCAGAG-3', 5'-AACCGAAGTCATAGCCACAC-3'.

Mouse lung epithelial cells (MLE-12) injury induced by BLM i*n vitro*.

Experiments were performed as descripted previously(39). Briefly, MLE-12 (ATCC company, Cat# CRL-2110) were seeded at $1X10^6$ cells per 60-mm dish and cultured in medium supplied with 2% FBS, 0.005mg/ml insulin (Sigma, Cat# 10516), 0.01mg/ml Tranferrin (Sigma, Cat# T8158), 30nM Sodium selenite (Sigma, Cat# S5261), 10nM Hydrocortisone (Sigma, Cat#H6909), 10nM Beta-estradiol (Sigma, Cat# E2758), 10mM HEPES (FisherBiotech, Cat# H0887), overnight. The cells were treated with PBS or BLM (50ug/ml) for 24h. The cells were washed and co-cultured with PBS, wild-type TSCs, or HO-1 null TSCs for 16h. The cells were collected for staining using the FITC Annexin V Apoptosis Detection kit (BD Pharmingen Cat# 556547), following the manufacturer's protocol, and then flow cytometry assessment (BD FACS Canto II) was performed. The data was analyzed using FlowJo software (TreeStar). AnnexinV and 7-Aminoactinomycin label the early and late apoptotic cells, respectively.

Statistics

One-way analysis of variance was performed when more than two groups were analyzed (Figure 1c, Figure 2, Figure 3b, Figure 4). For comparisons between two groups, we used Student's unpaired *t* test (Figure 5c, Figure 6b). Statistical significance was accepted at $P<0.05$.

Results

Transplantation of TSCs attenuates inflammation in ALI.

Intratracheal BLM in mice causes ALI within the first 7 days of exposure(34, 35). We hypothesized that transplantation of TSCs would have a benefit to decrease the injurious effect of BLM. To address this, we intratracheally administrated BLM at a dose of 0.75mg/kg in 100μl PBS (ALI), or the same volume of PBS (sham) into 8~10 weeks C57BL/6 male mice. At day 3 after exposure to BLM, mice received PBS, FBs or TSCs (both cells were pre-labeled with PKH67 green fluorescence), via the intratracheal route. The lungs were harvested for histology and BALF was collected at day 7 after exposure to BLM. To assess the ALI, lung sections were stained for hematoxylin and eosin (Figure 1a). The lungs of mice exposed to BLM and then receiving PBS or FBs showed more inflammatory cell infiltration and more alveolar damage, compared with sham mice receiving PBS. In contrast, the lungs of ALI mice that received TSCs revealed much less cellularity and less alveolar damage than mice receiving PBS or FB. Additionally, immunostaining for CD45, a marker of inflammatory cells, confirmed that

intratracheal exposure to BLM resulted in an increase in CD45 positive cells infiltrating in the lungs, compared with sham, while there were significantly less CD45 positive cells in the lungs of ALI mice that received TSCs compared with ALI mice receiving PBS or FBs(Figure 1b).

We next examined total cell counts and types of innate immune cells in BALF. BLM exposure increased the total cell counts in BALF from ALI mice receiving PBS or FBs compared with the sham. Intratracheal transplantation of TSCs significantly decreased the total cell counts in BALF, compared with ALI mice that received PBS or FBs (Figure 1c, left graph). Infiltration of neutrophils and macrophages into the acutely injured lungs of mice after intratracheal exposure to BLM is well described(40, 41). Thus, BAL cells were assessed using cytospins and Wright-Giemsa staining. The total macrophage counts in BALF from ALI mice that received PBS or FBs were significantly increased compared with sham, while ALI mice that received TSCs had a decrease in macrophage counts compared with ALI mice receiving PBS or FBs (Figure 1c, middle graph). The total neutrophil counts in BALF from ALI mice treated with TSCs were comparable to sham, and significantly less than that of ALI mice that received FBs (Figure 1c, right graphs). Taken together, these data demonstrate that intratracheal transplantation of TSCs reduced the inflammatory response, including the reduction of neutrophils and macrophages infiltrating into the acutely injured lungs of mice exposed to BLM.

Transplantation of TSCs attenuates proinflammation cytokines/chemokines in ALI.

In response to BLM-induced ALI, neutrophils, macrophages, alveolar epithelial cells and endothelial cells secrete proinflammatory cytokines and chemokines(42-45). Thus, we additionally investigated whether TSCs mediated the inflammatory response to ALI induced by BLM exposure. Total RNA was isolated from lungs and qRT-PCR was performed for IL-6, MCP-1 and KC. IL-6 is a marker of inflammation in the injury phase of ALI(44, 45). Intratracheal exposure to BLM significantly increased IL-6 expression in the lungs of ALI mice receiving PBS and FB compared with sham lungs. Interestingly, the level of IL-6 expression decreased in the lungs of ALI mice receiving TSCs, compared with ALI mice receiving FBs (Figure 2a, left panel). MCP-1, one of the key chemokines that regulate migration and infiltration of monocytes/macrophages(43), was increased in ALI, while administration of TSCs significantly decreased MCP-1 expression compared with lungs of ALI mice that received PBS or FBs (Figure 2a, middle panel). KC, a factor contributing to neutrophil recruitment to the lungs(42), also was increased in the lungs of mice exposed to BLM. However, mice treated with TSCs after ALI showed a decrease in the level of KC compared with lungs of mice receiving FB (Figure 2a, right panel). Furthermore. BALF was collected from sham and ALI mice, and assessed by ELISA. BALF IL-6 was undetectable in sham and

increased in mice exposed to BLM that received PBS or FBs. Intratracheal transplantation of TSCs reduced the level of BALF IL-6 compared with mice that received PBS after ALI, and a trend for a decrease compared with the FB group (Figure 2b, left panel). MCP-1 was also undetectable in BALF of the sham mice and increased in ALI mice receiving PBS and FBs. The intratracheal transplantation of TSCs significantly decrease the level of BALF MCP-1, compared with mice that received FB after BLM, and there was a trend of a decrease compared with mice that received PBS (Figure 2b, right panel).

TSCs protect lung epithelial cells from apoptosis after exposure to BLM *in vivo and vitro.*

The death of alveolar epithelial cells has been observed in ALI induced by BLM(39, 46). To assess the role of TSC in protection of the alveolar epithelial cells from apoptosis during ALI induced by BLM, we stained the lungs for cell death, using TUNEL (Figure 3). Apoptotic cells were frequently observed in the lungs at 7 days after intratracheal exposure to BLM in mice that received PBS or FBs, and rarely seen in the lungs of sham mice receiving PBS. Transplantation of TSCs into the lungs of mice after exposure to BLM showed a significant decrease in apoptotic cells compared with ALI mice receiving PBS and FBs (Figure 3a and 3b). These data demonstrate that TSCs play a role in protecting the lungs from cell death due to BLM.

The previous data (Figure 1 and 2) demonstrated that intratracheal transplantation of TSCs reduced inflammatory cell infiltrates and the level of pro-inflammatory cytokines, which may contribute to a decrease in cell death. To understand whether TSCs may have a direct role in protecting alveolar epithelial cells, independent of immune cells and cytokines, we performed apoptosis assays *in vitro* (Figure 4). MLE-12 were treated with PBS or BLM (50ug/ml) for 24h and were then co-cultured with PBS or TSCs for 16 hours. Cells were harvested and stained for Sca-1, which is present in 99% of TSCs (29) and not expressed in MLE-12, to exclude TSCs in the flow cytometry analysis for apoptosis (Additional file 1, upper left). MLE-12 were gated to assay for apoptotic cells (Additional file 1, upper middle and right). BLM exposure significantly increased the apoptosis of MLE-12 to 25.91±1.8%, compared with 14.31±1.4 % at baseline, while BLM-injured MLE-12 co-cultured with TSCs, demonstrated a significant decrease in apoptotic cell counts to 17.78±0.6% (Figure 4a, Additional file 1, lower panels). These data suggest TSCs directly protect lung epithelial cells from death induced by BLM.

To further understand this protective effect of TSCs, we explored the importance of heme oxygenase-1 (HO-1), a known cytoprotective molecule that has been reported to be important in the response of trophoblast cells to oxidative stress(47). Interestingly, TSCs harvested from the placentas of HO-1 deficient (HO-$1^{-/-}$) mice compared with HO-1 wild-type (HO-$1^{+/+}$) mice revealed that the protective role of TSCs against BLM-induced MLE-12 death

was lost in HO-1$^{-/-}$ cells, with a level of apoptosis greater than HO-1$^{+/+}$ cells (Figure 4b, Additional file 2). In fact, the level of MLE-12 death due to BLM was comparable in the group receiving HO-1$^{-/-}$ TSCs as to the group receiving no cells.

TSCs possess properties of self-renewal and differentiation into lung alveolar epithelial cells *in vitro.*

Beyond mediating the inflammatory and injury response associated with ALI due to BLM, we next wanted to understand whether TSCs are capable of engrafting and differentiating during ALI. We first investigated *in vitro* the property of self-renewal and differentiation of TSCs into lung alveolar epithelial cells**.** The TSCs were cultured at a limiting diluted in 100mm dish (density of one cell every 60 mm^2). After 14 days, clones formed from single cells (Figure 5a upper left), and the efficiency of clone formation was 21.3±3.09% (n=3). The clones were immunofluorescence stained for CD117, and these data demonstrated that the majority of clonal cells continued to express CD117 (Figure 5a upper right), demonstrating that the TSCs possess the stem cell properties of clonogenesis and self-renewal.

TSCs were next cultured in differentiation medium for lung alveolar epithelial cells, on an air-liquid interphase for 16~18 days. These cells were immunofluorescence stained for APQ5 (Figure 5b, upper row) or SPC (Figure 5b, lower row), markers for lung alveolar epithelial type I and II cells,

respectively. We found that the majority of the cells changed to a cobblestone-shape and expressed AQP5 and SPC. Total RNA was isolated from these cells and we also performed qRT-PCR for AQP5 and SPC. qRT-PCR revealed ~4-fold and ~5-fold greater mRNA levels of AQP5 and SPC respectively in the differentiated versus the undifferentiated cells (Figure 5c). These data demonstrate that TSCs possess the ability to differentiate into lung alveolar epithelial type I and II cells *in vitro.*

Transplanted TSCs engraft and differentiate into alveolar epithelial cells during ALI *in vivo*.

Male 8~10 weeks C57BL/6 mice received PBS (sham) or BLM (ALI) intratracheally. At day 3 after exposure to BLM, TSCs or FBs were pre-labeled with PKH67 fluorescence dye (green), and then TSCs or FBs were intratracheally administrated to ALI mice. The mice were sacrificed and the lungs were harvested at day 7 after exposure to BLM, for histologic assessment. Mouse lungs were sectioned (5μm) and images were taken by fluorescent microscopy for an assessment of engraftment (Figure 6a). No FITC positive cells were observed in sham mice receiving PBS (Figure 6a, upper row). FITC positive cells (TSCs or FBs pre-labeled with green) were observed in the distal lung of mice receiving BLM and subsequently transplanted with TSCs (green), but were less frequently seen in the lungs of ALI mice receiving FBs (Figure 6a, bottom and middle rows, respectively).

Single cell suspensions of lung tissue were also harvested to quantitate engraftment of TSCs by flow cytometery (Figure 6b). 1.54±0.9% of total lung cells were found to be exogenous TSCs that engrafted in the lungs of ALI mice (day 4 after TSC administration), which was significantly greater compared with that of ALI mice that received FBs with 0.43±0.2% green cells (Figure 6b).

To further understand the fate of transplanted TSCs *in vivo*, the lung sections were stained for AQP5 and SPC (Figure 7a). Images showed that some green fluorescent cells expressed either APQ5 (Figure 7a, white arrowheads, upper row) or SPC (Figure 7a, white arrowheads, lower row), while others remained positive for green fluorescent dye and did not express AQP5 or SPC (Figure 7a, white arrows). For quantitation of the subpopulations of exogenous green cells, the single cell suspension from the lung was stained for AQP5 or SPC and then run for flow cytometry. In the total engrafted cells, 21.38±3.9% and 26.32±9.9% of green cells expressed AQP5 and SPC, respectively (Figure 7b). These data revealed that TSCs were able to engraft and differentiate into alveolar epithelial cells during ALI.

Discussion

ALI is a devastating disease process with substantial morbidity and mortality and limited therapeutic options, with no treatments targeting disease pathobiology(1, 2). Inflammation and death of alveolar epithelial cells are the

two major initiating factors of this disease process, which leads to the high-protein fluid accumulating in lungs and ineffectively gas exchange resulting in ARDS. The use of stem cells as a potential treatment strategy for ALI is an evolving field of investigation. Although MSCs from various sources and alveolar epithelial cells have been shown to have therapeutic potential in rodent lung injury models, there is no evidence of these exogenous stem cells populating the lung alveolar epithelium *in vivo*(5, 24-26). Studies have reported the ability of murine ESCs and iPSCs to engraft and differentiate into alveolar epithelial cells *in vitro* and *in vivo(7-9)*. However, immunogenicity of these cells and ethical issues with ESCs represent barriers to their clinical application. In the present study, we demonstrate that intratracheal administration of TSCs in an experimental model of ALI led to a decrease in the injury response to BLM, including reduced infiltration of inflammatory cells and decreased production of pro-inflammatory cytokines in lung tissue and BALF. Furthermore, TSCs transplantation also protected alveolar epithelial cells from death, and engrafted in the injured lungs. These data suggest that TSCs, a placenta-derived stem cell easily obtained from discarded tissue, can be a potential future therapeutic option for ALI.

ALI in the early stage after exposure to BLM (within 7 days) is characterized by an extensive infiltration of inflammatory cells into the lung(40-42, 48). When mice received TSCs intratracheally 3 days after BLM exposure, at day 7 there was a significant decrease in $CD45^+$ cells compared

with mice receiving PBS or FBs (Figure 1). This was also demonstrated in BALF, in which not only total leukocytes, but macrophages and neutrophils were significantly less in the lungs of mice that received TSCs. In ALI, macrophages and neutrophils are recruited to the injured lungs by proinflammatory chemokines and cytokines, released from various cells, such as the epithelial and endothelial cells, and as well as macrophages and neutrophils(42-45). IL-6 is considered to be an important proinflammatory cytokine and a biomarker of poor outcome in ALI(44, 45). MCP-1 is one of the key chemokines that regulate migration and infiltration of monocytes/macrophages(43), and KC is one of the major chemokines contributing to neutrophil recruitment to the lung(42). Our data demonstrated a significant decrease in the expression of IL-6, MCP-1 and KC in the lungs, and reduced levels of IL-6 and MCP-1 in BALF, from the lungs of ALI mice that received TSCs, compared with mice receiving PBS or FBs. This study for the first time demonstrates that TSCs are capable of decreasing the expression and production of chemokines and cytokines in BLM-induced ALI (Figure 2), resulting in a reduced infiltration of macrophages and neutrophils into the lungs. These date support TSCs have anti-inflammatory properties *in vivo*.

The mechanism of BLM-induced ALI is not fully understood, but numerous studies have shown that the exposure of lungs to BLM may directly trigger a series of oxidative reactions leading to cell death(40, 41). Alveolar epithelial

cell injury and death are further aggravated by the infiltration of inflammatory cells into the lung. As a treatment for ALI, it is important to protect alveolar epithelial cells from death. Our data showed the intratracheal transplantation of TSCs into mice with BLM-induced ALI reduced the death of cells in the lungs, compared with mice exposed to BLM receiving PBS or FBs (Figure 3). This likely occurred in part by decreasing the inflammatory response in the lungs, both production of cytokines and chemokines and also infiltration of macrophages and neutrophils. In order to understand whether TSCs play the role in directly protecting the alveolar epithelial cells from apoptosis, we performed *in vitro* experiments to exclude the effects of proinflammatory mediators and immune cells. MLE-12 were injured by BLM exposure, and then co-cultured with TSCs. Flow cytometry analysis for cell apoptosis showed that TSCs protected MLE-12 from BLM-induced apoptosis *in vitro*, suggesting TSCs play a role in directly protecting the pulmonary cells from death (Figure 4). Furthermore, we demonstrated that production of HO-1 in TSCs contributed to this response, as TSCs lacking HO-1 lost the ability to protect lung epithelial cells from BLM-induced death. HO-1 and its downstream production of carbon monoxide (CO), by catabolizing heme, have previously been shown to play a protective role against ALI from a variety of insults (49, 50). In fact, clinical trials are ongoing for the use of low-dose inhaled CO for the treatment of patients with ARDS(51).

Beyond the impact of TSCs on inflammation and death of lung alveolar epithelial cells, we also investigated the ability of TSCs to engraft and differentiate into lung alveolar epithelial cells after the onset of injury. At 3 days after exposure to BLM, TSCs were intratracheally transplanted into mice, and assessment of lung engraftment was performed 4 days later. Approximately 1.5% of lung cells were derived from exogenous TSCs (Figure 6). Some of these exogenous cells stained positive for either APQ5 or SPC, markers of alveolar epithelial type I or type II cells, respectively. In the population exogenously labeled TSCs that engrafted, 23% expressed AQP5 and 26% expressed SPC (Figure 7). These results suggest that TSCs were able to survive after intratracheal transplantation into the injured lungs, and more than half of the surviving cells differentiated into alveolar epithelial type I and II cells. Whether the engraftment of TSCs in the lungs after BLM exposure contributed to the reduction of injury requires further investigation, however this study demonstrates that TSCs have the potential to engraft during ALI.

Conclusions

Taken together, our data provide preclinical evidence that TSCs may have future clinical application in ALI by decreasing the inflammatory response, reducing the death of lung alveolar epithelial cells, and engrafting with the potential for differentiation and replacement of injured cells in the lung.

Abbreviations

ALI: Acute lung injury

AQP5: Aquaporin 5

ARDS: Acute respiratory distress syndrome

BALF: Bronchoalveolar lavage fluid

BLM: Bleomycin

CO: Carbon monoxide

DAPI: 4′,6-diamidino-2-phenylindole

ELISA: Enzyme-linked immunosorbent assay

ESCs: Embryonic stem cells

FBs: Fibroblasts

HO-1: Heme oxygenase-1

IL-6: Interleukin 6

iPSCs: Induced pluripotent stem cells

MLE-12: Mouse lung epithelial cells

MSCs: Mesenchymal stem/stromal cells

MCP-1: Monocyte chemoattractant protein-1

KC: Keratinocyte-derived chemokine

qRT-PCR: Real-time polymerase chain reaction

SPC: Prosurfactant protein C

TSCs: Trophoblast stem cells

TUNEL: Terminal deoxynucleotidyl transferase dUTP nick end labeling

Declarations

Ethics approval and consent to participate

The use of mice and the studies performed were carried out in accordance with the Public Health Service policy on the humane care and use of laboratory animals, and the protocol was approved by the Institutional Animal Care and Use Committee of Brigham and Women's Hospital.

Consent for publication

Not applicable.

Availability of data and materials

The original data are available from the corresponding author on request.

Competing interests

The authors declare that they have no competing interests.

Funding

This work was supported by Scientist Development Grant 11SDG7220018 from the American Heart Association (X.L.) and National Institutes of Health grant U01AI38318 (M.A.P.).

Author's Contributions

JH, GL and MH contributed to the collection and assembly of data, data analysis, and interpretation. MY, KX and XL contributed to the collection and assembly of data. ET, YS, AM, SK, SE and IOR contributed to the design. MAP and XL contributed to the conception and design, manuscript writing, data analysis, and interpretation. All authors read and approved the final manuscript.

Acknowledgments

We thank Bonna Ith for his assistance with tissue processing, embedding, and sectioning for immunostaining analyses; and Dr. Ehab Ayaub for his expertise and recommendations regarding the bleomycin model of lung injury.

Affiliations

Department of Medicine, Division of Pulmonary and Critical Care Medicine, Brigham and Women's Hospital, Boston, MA USA,

Department of Pediatrics, Division of Newborn Medicine, Boston Children's Hospital, Boston, MA, USA,

Department of Medicine, Division of Pulmonary, Critical Care and Sleep Medicine, Baylor College of Medicine

School of Life Sciences, Beijing University of Chinese Medicine, Beijing, China

Department of Pediatric Newborn Medicine, Brigham and Women's Hospital, Boston, MA, USA

Corresponding author

Correspondence to xlliu@rics.bwh.harvard.edu

Publisher's note

References

1. Johnson ER, Matthay MA. Acute lung injury: epidemiology, pathogenesis, and treatment. J Aerosol Med Pulm Drug Deliv. 2010;23(4):243-52.
2. Rubenfeld GD, Caldwell E, Peabody E, Weaver J, Martin DP, Neff M, et al. Incidence and outcomes of acute lung injury. N Engl J Med. 2005;353(16):1685-93.
3. Lee JH, Park J, Lee JW. Therapeutic use of mesenchymal stem cell-derived extracellular vesicles in acute lung injury. Transfusion. 2019;59(S1):876-83.
4. Lee JW, Fang X, Krasnodembskaya A, Howard JP, Matthay MA. Concise review: Mesenchymal stem cells for acute lung injury: role of paracrine soluble factors. Stem Cells. 2011;29(6):913-9.

5. Araujo IM, Abreu SC, Maron-Gutierrez T, Cruz F, Fujisaki L, Carreira H, Jr., et al. Bone marrow-derived mononuclear cell therapy in experimental pulmonary and extrapulmonary acute lung injury. Crit Care Med. 2010;38(8):1733-41.
6. Matthay MA, Goolaerts A, Howard JP, Lee JW. Mesenchymal stem cells for acute lung injury: preclinical evidence. Crit Care Med. 2010;38(10 Suppl):S569-73.
7. Soh BS, Zheng D, Li Yeo JS, Yang HH, Ng SY, Wong LH, et al. CD166(pos) subpopulation from differentiated human ES and iPS cells support repair of acute lung injury. Mol Ther. 2012;20(12):2335-46.
8. Wang D, Morales JE, Calame DG, Alcorn JL, Wetsel RA. Transplantation of human embryonic stem cell-derived alveolar epithelial type II cells abrogates acute lung injury in mice. Mol Ther. 2010;18(3):625-34.
9. Wilson JG, Liu KD, Zhuo H, Caballero L, McMillan M, Fang X, et al. Mesenchymal stem (stromal) cells for treatment of ARDS: a phase 1 clinical trial. Lancet Respir Med. 2015;3(1):24-32.
10. Yang KY, Shih HC, How CK, Chen CY, Hsu HS, Yang CW, et al. IV delivery of induced pluripotent stem cells attenuates endotoxin-induced acute lung injury in mice. Chest. 2011;140(5):1243-53.
11. Yin X, Liang Z, Yun Y, Pei L. Intravenous Transplantation of BMP2-Transduced Endothelial Progenitor Cells Attenuates Lipopolysaccharide-

Induced Acute Lung Injury in Rats. Cell Physiol Biochem. 2015;35(6):2149-58.

12. Liu KD, Wilson JG, Zhuo H, Caballero L, McMillan ML, Fang X, et al. Design and implementation of the START (STem cells for ARDS Treatment) trial, a phase 1/2 trial of human mesenchymal stem/stromal cells for the treatment of moderate-severe acute respiratory distress syndrome. Ann Intensive Care. 2014;4:22.
13. Zheng G, Huang L, Tong H, Shu Q, Hu Y, Ge M, et al. Treatment of acute respiratory distress syndrome with allogeneic adipose-derived mesenchymal stem cells: a randomized, placebo-controlled pilot study. Respir Res. 2014;15:39.
14. Phinney DG, Prockop DJ. Concise review: mesenchymal stem/multipotent stromal cells: the state of transdifferentiation and modes of tissue repair--current views. Stem Cells. 2007;25(11):2896-902.
15. Rojas M, Xu J, Woods CR, Mora AL, Spears W, Roman J, et al. Bone marrow-derived mesenchymal stem cells in repair of the injured lung. Am J Respir Cell Mol Biol. 2005;33(2):145-52.
16. Zacharias WJ, Frank DB, Zepp JA, Morley MP, Alkhaleel FA, Kong J, et al. Regeneration of the lung alveolus by an evolutionarily conserved epithelial progenitor. Nature. 2018;555(7695):251-5.
17. Antoniadou E, David AL. Placental stem cells. Best Pract Res Clin Obstet Gynaecol. 2016;31:13-29.

18. Parolini O, Caruso M. Review: Preclinical studies on placenta-derived cells and amniotic membrane: an update. Placenta. 2011;32 Suppl 2:S186-95.
19. Pipino C, Shangaris P, Resca E, Zia S, Deprest J, Sebire NJ, et al. Placenta as a reservoir of stem cells: an underutilized resource? Br Med Bull. 2013;105:43-68.
20. Pogozhykh O, Prokopyuk V, Figueiredo C, Pogozhykh D. Placenta and Placental Derivatives in Regenerative Therapies: Experimental Studies, History, and Prospects. Stem Cells Int. 2018;2018:4837930.
21. Roura S, Pujal JM, Galvez-Monton C, Bayes-Genis A. The role and potential of umbilical cord blood in an era of new therapies: a review. Stem Cell Res Ther. 2015;6:123.
22. Park TS, Gavina M, Chen CW, Sun B, Teng PN, Huard J, et al. Placental perivascular cells for human muscle regeneration. Stem Cells Dev. 2011;20(3):451-63.
23. Mathews S, Lakshmi Rao K, Suma Prasad K, Kanakavalli MK, Govardhana Reddy A, Avinash Raj T, et al. Propagation of pure fetal and maternal mesenchymal stromal cells from terminal chorionic villi of human term placenta. Sci Rep. 2015;5:10054.
24. Yuan W, Song HY, Xiong J, Jiang WL, Kang GJ, Huang J, et al. Placentaderived mesenchymal stem cells ameliorate

lipopolysaccharideinduced inflammation in RAW264.7 cells and acute lung injury in rats. Mol Med Rep. 2020.

25. Hodges RJ, Lim R, Jenkin G, Wallace EM. Amnion epithelial cells as a candidate therapy for acute and chronic lung injury. Stem Cells Int. 2012;2012:709763.

26. Murphy S, Lim R, Dickinson H, Acharya R, Rosli S, Jenkin G, et al. Human amnion epithelial cells prevent bleomycin-induced lung injury and preserve lung function. Cell Transplant. 2011;20(6):909-23.

27. Kim SY, Joglekar MV, Hardikar AA, Phan TH, Khanal D, Tharkar P, et al. Placenta Stem/Stromal Cell-Derived Extracellular Vesicles for Potential Use in Lung Repair. Proteomics. 2019;19(17):e1800166.

28. Natale BV, Schweitzer C, Hughes M, Globisch MA, Kotadia R, Tremblay E, et al. Sca-1 identifies a trophoblast population with multipotent potential in the mid-gestation mouse placenta. Sci Rep. 2017;7(1):5575.

29. Hou M, Han J, Li G, Kwon MY, Jiang J, Emani S, et al. Multipotency of mouse trophoblast stem cells. Stem Cell Res Ther. 2020;11(1):55.

30. Carr DH. An experimental study of trophoblast growth in the lung. Obstet Gynecol. 1977;50(4):473-8.

31. Calo G, Sabbione F, Vota D, Paparini D, Ramhorst R, Trevani A, et al. Trophoblast cells inhibit neutrophil extracellular trap formation and enhance apoptosis through vasoactive intestinal peptide-mediated pathways. Hum Reprod. 2017;32(1):55-64.

32. Fraccaroli L, Grasso E, Hauk V, Paparini D, Soczewski E, Mor G, et al. VIP boosts regulatory T cell induction by trophoblast cells in an in vitro model of trophoblast-maternal leukocyte interaction. J Leukoc Biol. 2015;98(1):49-58.
33. Ramhorst R, Calo G, Paparini D, Vota D, Hauk V, Gallino L, et al. Control of the inflammatory response during pregnancy: potential role of VIP as a regulatory peptide. Ann N Y Acad Sci. 2019;1437(1):15-21.
34. Rhee CK, Lee SH, Yoon HK, Kim SC, Lee SY, Kwon SS, et al. Effect of nilotinib on bleomycin-induced acute lung injury and pulmonary fibrosis in mice. Respiration. 2011;82(3):273-87.
35. Steffen L, Ruppert C, Hoymann HG, Funke M, Ebener S, Kloth C, et al. Surfactant replacement therapy reduces acute lung injury and collapse induration-related lung remodeling in the bleomycin model. Am J Physiol Lung Cell Mol Physiol. 2017;313(2):L313-L27.
36. Zhou Q, Ye X, Sun R, Matsumoto Y, Moriyama M, Asano Y, et al. Differentiation of mouse induced pluripotent stem cells into alveolar epithelial cells in vitro for use in vivo. Stem Cells Transl Med. 2014;3(6):675-85.
37. Yet SF, Perrella MA, Layne MD, Hsieh CM, Maemura K, Kobzik L, et al. Hypoxia induces severe right ventricular dilatation and infarction in heme oxygenase-1 null mice. J Clin Invest. 1999;103(8):R23-9.

38. Hall SR, Tsoyi K, Ith B, Padera RF, Jr., Lederer JA, Wang Z, et al. Mesenchymal stromal cells improve survival during sepsis in the absence of heme oxygenase-1: the importance of neutrophils. Stem Cells. 2013;31(2):397-407.
39. Lee VY, Schroedl C, Brunelle JK, Buccellato LJ, Akinci OI, Kaneto H, et al. Bleomycin induces alveolar epithelial cell death through JNK-dependent activation of the mitochondrial death pathway. Am J Physiol Lung Cell Mol Physiol. 2005;289(4):L521-8.
40. Williamson JD, Sadofsky LR, Hart SP. The pathogenesis of bleomycin-induced lung injury in animals and its applicability to human idiopathic pulmonary fibrosis. Exp Lung Res. 2015;41(2):57-73.
41. Su X, Liu K, Xie Y, Zhang M, Wang Y, Zhao M, et al. Protective effect of a polyphenols-rich extract from Inonotus Sanghuang on bleomycin-induced acute lung injury in mice. Life Sci. 2019;230:208-17.
42. Shah D, Romero F, Stafstrom W, Duong M, Summer R. Extracellular ATP mediates the late phase of neutrophil recruitment to the lung in murine models of acute lung injury. Am J Physiol Lung Cell Mol Physiol. 2014;306(2):L152-61.
43. Deshmane SL, Kremlev S, Amini S, Sawaya BE. Monocyte chemoattractant protein-1 (MCP-1): an overview. J Interferon Cytokine Res. 2009;29(6):313-26.

44. Cross LJ, Matthay MA. Biomarkers in acute lung injury: insights into the pathogenesis of acute lung injury. Crit Care Clin. 2011;27(2):355-77.
45. Bhargava M, Wendt CH. Biomarkers in acute lung injury. Transl Res. 2012;159(4):205-17.
46. Olajuyin AM, Zhang X, Ji HL. Alveolar type 2 progenitor cells for lung injury repair. Cell Death Discov. 2019;5:63.
47. Luan X, Yan Y, Zheng Q, Wang M, Chen W, Yu J, et al. Excessive reactive oxygen species induce apoptosis via the APPL1-Nrf2/HO-1 antioxidant signalling pathway in trophoblasts with missed abortion. Life Sci. 2020;254:117781.
48. White DA, Kris MG, Stover DE. Bronchoalveolar lavage cell populations in bleomycin lung toxicity. Thorax. 1987;42(7):551-2.
49. Fredenburgh LE, Baron RM, Carvajal IM, Mouded M, Macias AA, Ith B, et al. Absence of heme oxygenase-1 expression in the lung parenchyma exacerbates endotoxin-induced acute lung injury and decreases surfactant protein-B levels. Cell Mol Biol (Noisy-le-grand). 2005;51(5):513-20.
50. Ryter SW, Choi AM. Heme oxygenase-1/carbon monoxide: novel therapeutic strategies in critical care medicine. Curr Drug Targets. 2010;11(12):1485-94.

51. Fredenburgh LE, Perrella MA, Barragan-Bradford D, Hess DR, Peters E, Welty-Wolf KE, et al. A phase I trial of low-dose inhaled carbon monoxide in sepsis-induced ARDS. JCI Insight. 2018;3(23) e124039.

Figure legend

Figure 1. Administration of TSCs attenuates infiltration of inflammatory cells in ALI.

Male 8~10 weeks C57BL/6 mice received PBS (sham) or BLM 0.75mg/kg (ALI) intratracheally. At day 3 after BLM exposure, PBS, FBs, or TSCs were administrated intratracheally. The mice were sacrificed at day 7, and lung tissue and BALFs were collected. a) Representative images of Hematoxylin and Eosin staining of the lungs from sham mice (sham+PBS, upper left), and ALI mice that received PBS (ALI+PBS, upper right), FBs (ALI+FB, lower left) or TSCs (ALI+TSC, lower right). b) Representative images of immunostaining for CD45 (brown), from sham mice (Sham+PBS, upper left), and ALI mice that received PBS (ALI+PBS, upper right), FBs (ALI+FB, lower left) or TSCs (ALI+TSC, lower right). Methyl green counterstain (blue). c) BALFs were collected for assessment of total cell number and were cytospun for differential quantification of macrophages and neutrophils. Bar graphs show quantitation of total cells (left panel, n=5~6 for each group), macrophages (middle panel, n=3~6 for each group) and neutrophils (right panel, n=3~6 for each group) in BALF, from sham mice (sham+PBS, white bars), ALI mice that

received PBS (ALI+PBS, black bars), FBs (ALI+FB, light grey bars) or TSCs (ALI+TSC, dark grey bars). *P<0.05, versus sham group, &P<0.05, versus ALI+PBS group, $$P$<0.05, versus ALI+FB group, *#P=0.05* versus sham group.

Figure 2. Administration of TSCs alters the cytokine profile in ALI.

The lung tissue and BALFs were harvested and measured for pro-inflammatory cytokines by RT-PCR and ELISA. a) Quantitation of qRT-PCR for IL-6 (left panel), MCP-1 (middle panel) and KC (right panel) of lungs, from sham mice (white bars, n=6), and ALI mice that received PBS (black bars, n=9), FBs (light grey bars, n=8) or TSCs (dark grey bars, n=6). *P<0.001, versus sham group. & P<0.05, versus ALI+PBS group. $ P<0.005, versus ALI+FB group. b) Quantitation of ELISA for IL-6 and MCP-1 in BALF, from sham mice (undetectable, UD), ALI mice that received PBS (black bars), FBs (light grey bars) or TSCs (dark grey bars). & P<0.05, versus ALI+PBS group, $$P$<0.05, versus ALI+FB group, n=6~8 for each group.

Figure 3. Administration of TSCs protects apoptosis in ALI.

The lungs were stained for TUNEL. a) Representative images of immunofluorescence staining for TUNEL (green) and DAPI (blue) for nuclear, on lung sections, from sham mice (sham+PBS, upper left), ALI mice that received PBS (ALI+PBS, upper right), FBs (ALI+FB, lower left) or TSCs (ALI+TSC, lower right). b) Quantitation of TUNEL staining of the lung sections,

from sham mice (sham+PBS, white bar, n=9). ALI mice that received PBS (ALI+PBS, black bar, n=15), FBs (ALI+FB, light grey bar, n=18) or TSCs (ALI+TSC, dark grey bar, n=15). *P<0.0001, versus sham+PBS group, &P<0.0001, versus ALI+PBS group, $$P$<0.001, versus ALI+FB group.

Figure 4. TSCs protect MLE-12 from apoptosis induced by BLM *in vitro.* MLE-12 were treated with PBS or BLM, and then co-cultured with PBS or TSCs. a) Quantitation of flow cytometry assay. MLE-12 treated with PBS (MLE12, white bar), or BLM followed by PBS (MLE12+BLM, black bar) or TSCs (MLE12+BLM+TSC, light grey bar). n=3 for each group. b) Quantitation of flow cytometry assay showing MLE12 treated with PBS (MLE12, white bar), or BLM followed by PBS (MLE12+BLM, black bar), wild-type TSCs (MLE12+BLM+HO1$^{+/+}$TSCs, light grey bar) or HO-1 null TSCs (MLE12+BLM+HO1$^{-/-}$TSC, dark grey bar). *P<0.01 versus MLE12 group. &P<0.01 versus MLE12+BLM group. $P<0.05 versus MLE12+BLM+HO1$^{+/+}$TSCs group, n=3 for each group.

Figure 5. TSCs possess the capability of clone formation and differentiation into alveolar epithelial cells *in vitro.* TSCs were cultured in a 100-mm dish at limited dilution of one cell every 60 mm^2 for 14 days. a) Representative phase contrast images of an entire clone (left), and a clone immunofluorescence stained for CD117 (green, right). DAPI

demonstrates nuclear staining (blue). b) TSCs were cultured in epithelial cell differentiation medium on an air liquid interface for 16~18 days. Representative images of these differentiated cells immunofluorescence stained for AQP5 (red, upper row) and SPC (red, lower row), with merged images including nuclear staining for DAPI (blue, right upper and lower). c) Bar graph showing quantitation of qRT-PCR for AQP5 (right panel) and SPC (left panel) in fold change comparing differentiated (Diff, black bars) to undifferentiated cells (Undiff, white bars), * versus undifferentiated group, $P<0.001$ for AQP5, $P<0.05$ for SPC, n=5 for each group.

Figure 6. TSCs engraft in the lung injured by BLM.

Male 8~10 weeks C57BL/6 mice received PBS (sham) or BLM (ALI) intratracheally. At day 3 after BLM exposure, PBS, FBs, or TSCs were administrated intratracheally. The TSCs and FBs were dyed with PKH67 (green) prior to injection. The lungs were harvested at day 7 after BLM exposure. a) Representative images of the lung, from sham mice (sham+PBS, top row), ALI mice that received FB (ALI+FB, middle row) and TSCs (ALI+TSC, bottom row). Images showing $FITC^+$ cells (green, left column), and merged with nuclear staining for DAPI (blue, right column). White arrowheads point to engrafted cells (green). b) Representative scatter plots of flow cytometry showing the gating strategy: FITC negative (upper left) and PKH67 positive (upper right), $FITC^+$ cells from the lungs of ALI mice that received FBs

(ALI+FB, lower left) and TSCs (ALI+TSC, lower right). Bar graph represents quantitation of % green cells in the total lung suspension. *P<0.05, versus ALI+FB group. n=6 for ALI+FB and n=5 for ALI+TSC.

Figure 7. TSCs differentiate into alveolar epithelial cells in the lung injured by BLM.

TSCs were pre-labeled with PKH67 (green) and then intratracheally injected into the lungs at day 3 after BLM exposure. The lungs were harvested at day 7 for histologic assessment. a) Representative images of the lung immunofluorescence staining for AQP5 and SPC (red, middle column), TSC pre-labeled with PKH67 (green, left column), and merged images with nuclear staining for DAPI (blue, right column). White arrowheads point to green$^+$APQ5$^+$ and green$^+$SPC$^+$ cells (upper and lower rows, respectively). White arrows point to green$^+$AQP5$^-$and green$^+$SPC$^-$ cells (upper and lower rows, respectively). b) Representative scatter plots of flow cytometry showing the gating strategy (upper row), FITC$^+$ control from TSCs stained with PKH67 (first panel), FITC$^+$ TSCs gated from unstained cells of the lung that received PKH67-prelabeled TSCs (second panel), APC$^+$ gated from the population of FITC$^+$ cells in the second panel (third panel), and isotype control from the normal lung stained with FITC- and APC-isotypes (fourth panel). The lower row shows representative scatter plots of flow cytometry. The cells from BLM injured lungs receiving pre-labeled TSCs (FITC) and were stained for APQ5

or SPC (APC). The percentage of $FITC^+$ cells in the total lung cell population is shown in the gates (G+, lower row, the first and third panels), in which these cells gated for a percentage of $FITC^+AQP5^+$ and $FITC^+SPC^+$ in total $FITC^+$ cells (second and fourth panels, respectively). The pie graph shows quantitation of $FITC^+APQ5^+$ and $FITC^+SPC^+$ in the total $FITC^+$ cells. n=5 for each group.

Figures

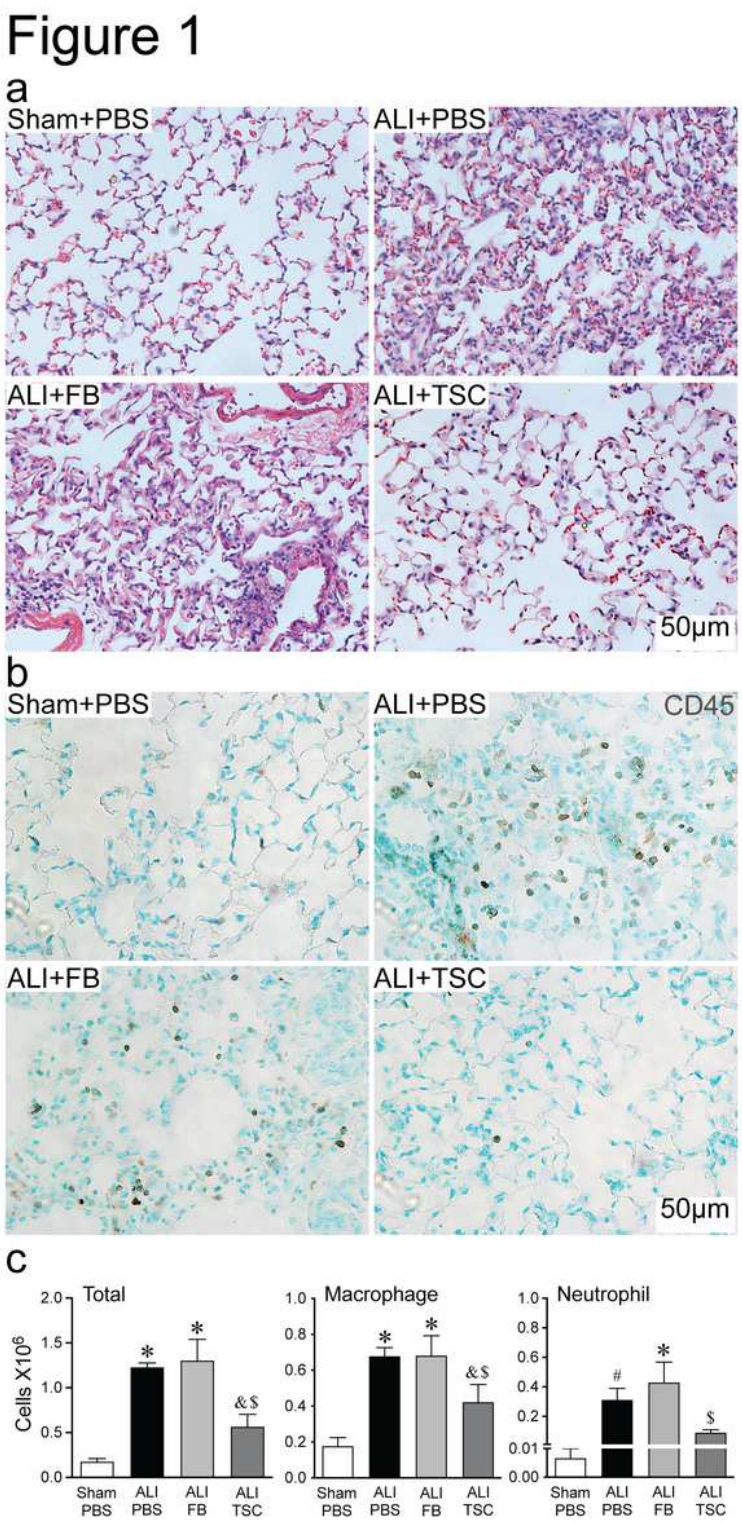

Figure 1

Administration of TSCs attenuates infiltration of inflammatory cells in ALI. Male 8~10 weeks C57BL/6 mice received PBS (sham) or BLM 0.75mg/kg (ALI) intratracheally. At day 3 after BLM exposure, PBS, FBs, or TSCs were administrated intratracheally. The mice were sacrificed at day 7, and lung tissue and

BALFs were collected. a) Representative images of Hematoxylin and Eosin staining of the lungs from sham mice (sham+PBS, upper left), and ALI mice that received PBS (ALI+PBS, upper right), FBs (ALI+FB, lower left) or TSCs (ALI+TSC, lower right). b) Representative images of immunostaining for CD45 (brown), from sham mice (Sham+PBS, upper left), and ALI mice that received PBS (ALI+PBS, upper right), FBs (ALI+FB, lower left) or TSCs (ALI+TSC, lower right). Methyl green counterstain (blue). c) BALFs were collected for assessment of total cell number and were cytospun for differential quantification of macrophages and neutrophils. Bar graphs show quantitation of total cells (left panel, n=5~6 for each group), macrophages (middle panel, n=3~6 for each group) and neutrophils (right panel, n=3~6 for each group) in BALF, from sham mice (sham+PBS, white bars), ALI mice that 40 received PBS (ALI+PBS, black bars), FBs (ALI+FB, light grey bars) or TSCs (ALI+TSC, dark grey bars). *P<0.05, versus sham group, &P<0.05, versus ALI+PBS group, $P<0.05, versus ALI+FB group, #P=0.05 versus sham group.

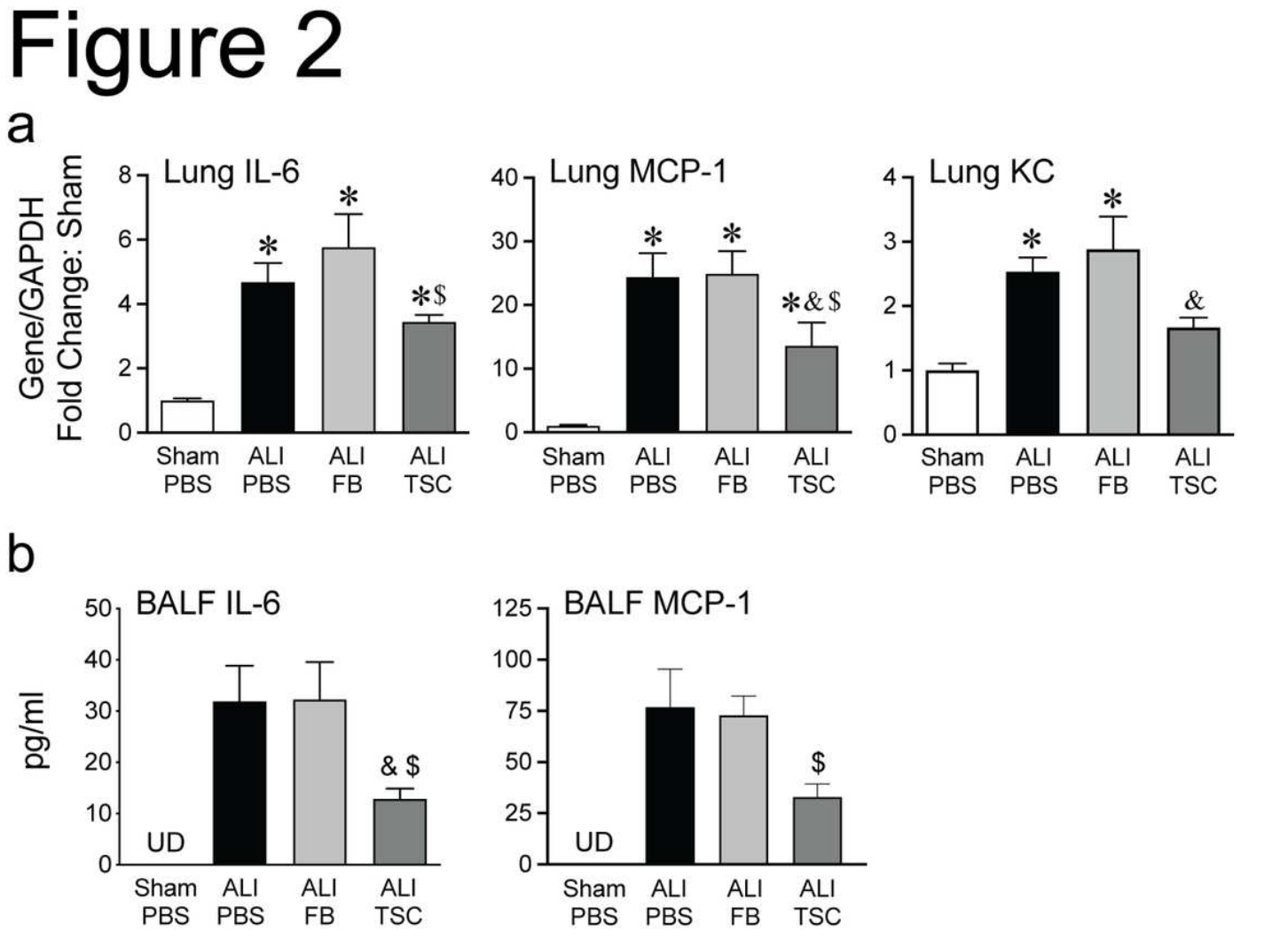

Figure 2

Administration of TSCs alters the cytokine profile in ALI. The lung tissue and BALFs were harvested and measured for pro inflammatory cytokines by RT-PCR and ELISA. a) Quantitation of qRT-PCR for IL-6 (left panel), MCP-1 (middle panel) and KC (right panel) of lungs, from sham mice (white bars, n=6), and ALI

mice that received PBS (black bars, n=9), FBs (light grey bars, n=8) or TSCs (dark grey bars, n=6). *P<0.001, versus sham group. & P<0.05, versus ALI+PBS group. $ P<0.005, versus ALI+FB group. b) Quantitation of ELISA for IL-6 and MCP-1 in BALF, from sham mice (undetectable, UD), ALI mice that received PBS (black bars), FBs (light grey bars) or TSCs (dark grey bars). & P<0.05, versus ALI+PBS group, $P<0.05, versus ALI+FB group, n=6~8 for each group.

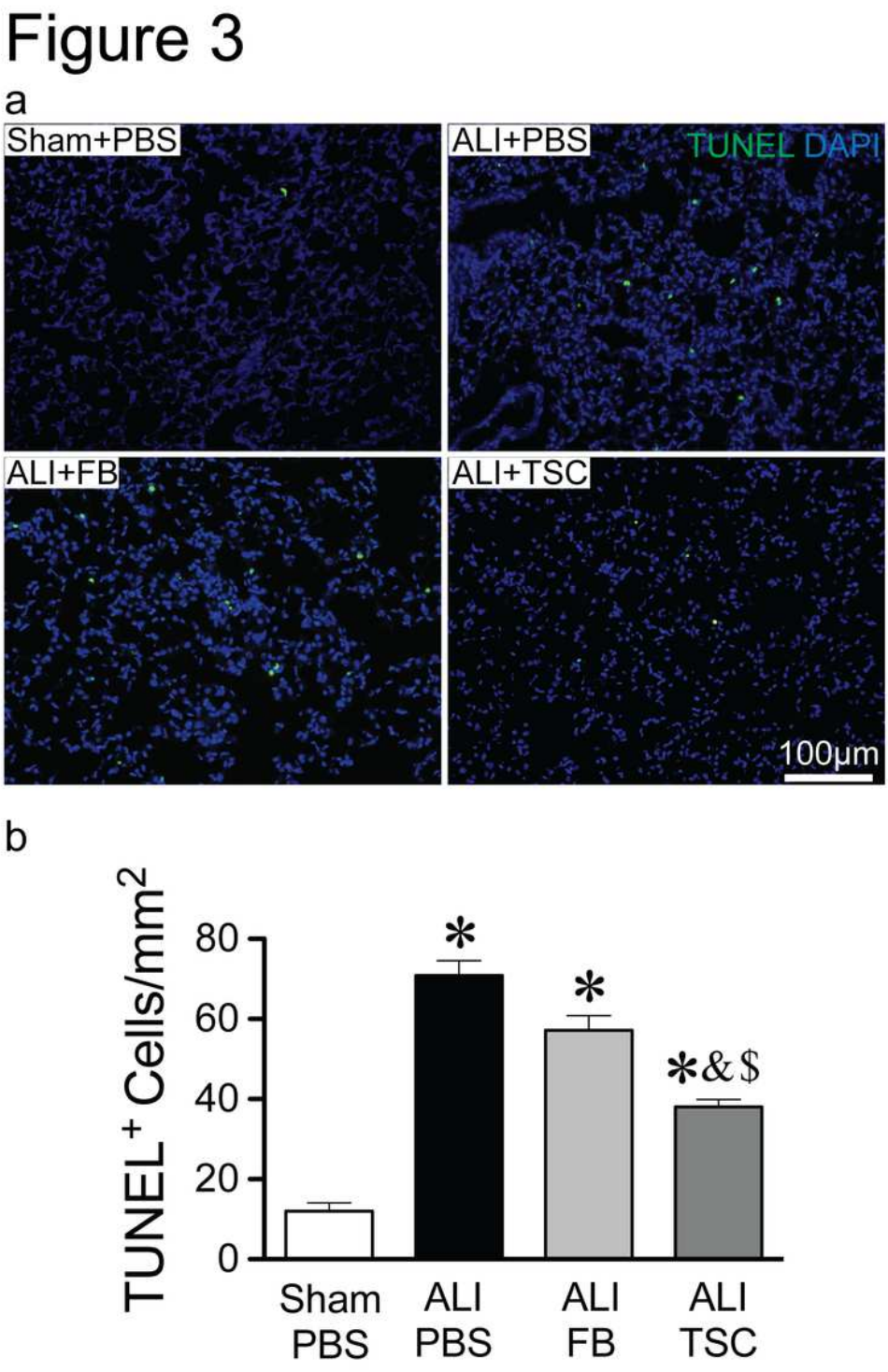

Figure 3

Administration of TSCs protects apoptosis in ALI. The lungs were stained for TUNEL. a) Representative images of immunofluorescence staining for TUNEL (green) and DAPI (blue) for nuclear, on lung sections, from sham mice (sham+PBS, upper left), ALI mice that received PBS (ALI+PBS, upper right), FBs (ALI+FB, lower left) or TSCs (ALI+TSC, lower right). b) Quantitation of TUNEL staining of the lung sections, 41 from sham mice (sham+PBS, white bar, n=9). ALI mice that received PBS (ALI+PBS, black bar, n=15), FBs (ALI+FB, light grey bar, n=18) or TSCs (ALI+TSC, dark grey bar, n=15). *P<0.0001, versus sham+PBS group, &P<0.0001, versus ALI+PBS group, $P<0.001, versus ALI+FB group.

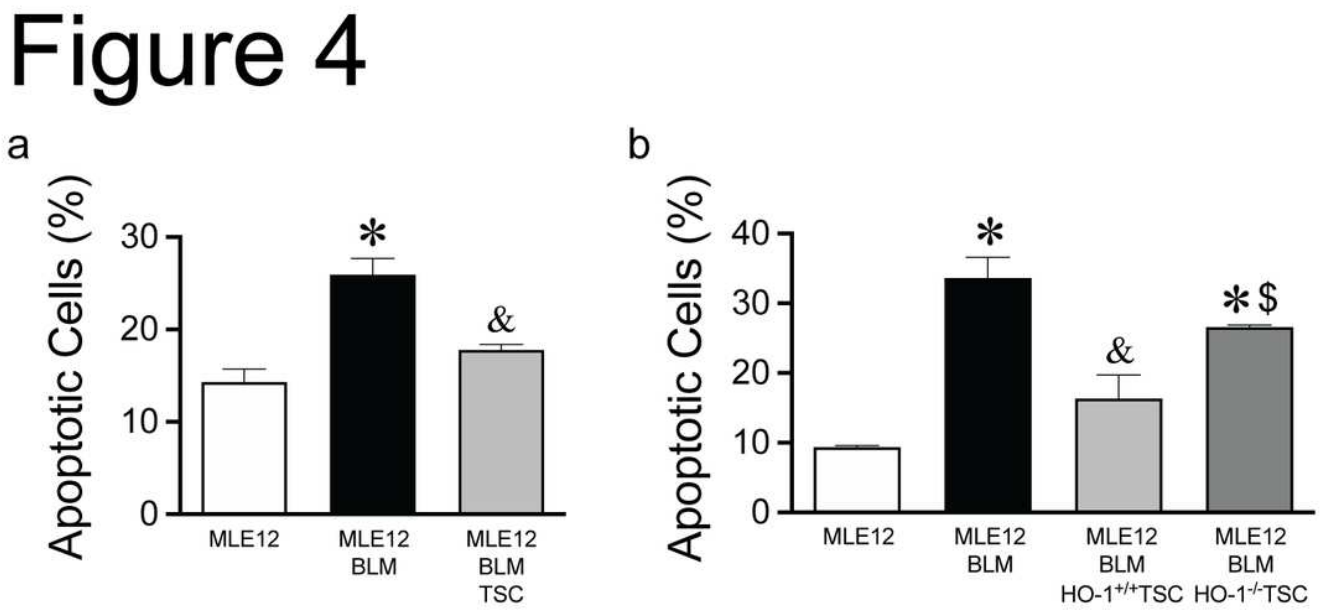

Figure 4

TSCs protect MLE-12 from apoptosis induced by BLM in vitro. MLE-12 were treated with PBS or BLM, and then co-cultured with PBS or TSCs. a) Quantitation of flow cytometry assay. MLE-12 treated with PBS (MLE12, white bar), or BLM followed by PBS (MLE12+BLM, black bar) or TSCs (MLE12+BLM+TSC, light grey bar). n=3 for each group. b) Quantitation of flow cytometry assay showing MLE12 treated with PBS (MLE12, white bar), or BLM followed by PBS (MLE12+BLM, black bar), wild-type TSCs (MLE12+BLM+HO1+/+ TSCs, light grey bar) or HO-1 null TSCs (MLE12+BLM+HO1-/- TSC, dark grey bar). *P<0.01 versus MLE12 group. &P<0.01 versus MLE12+BLM group. $P<0.05 versus MLE12+BLM+HO1+/+ TSCs group, n=3 for each group.

Figure 5

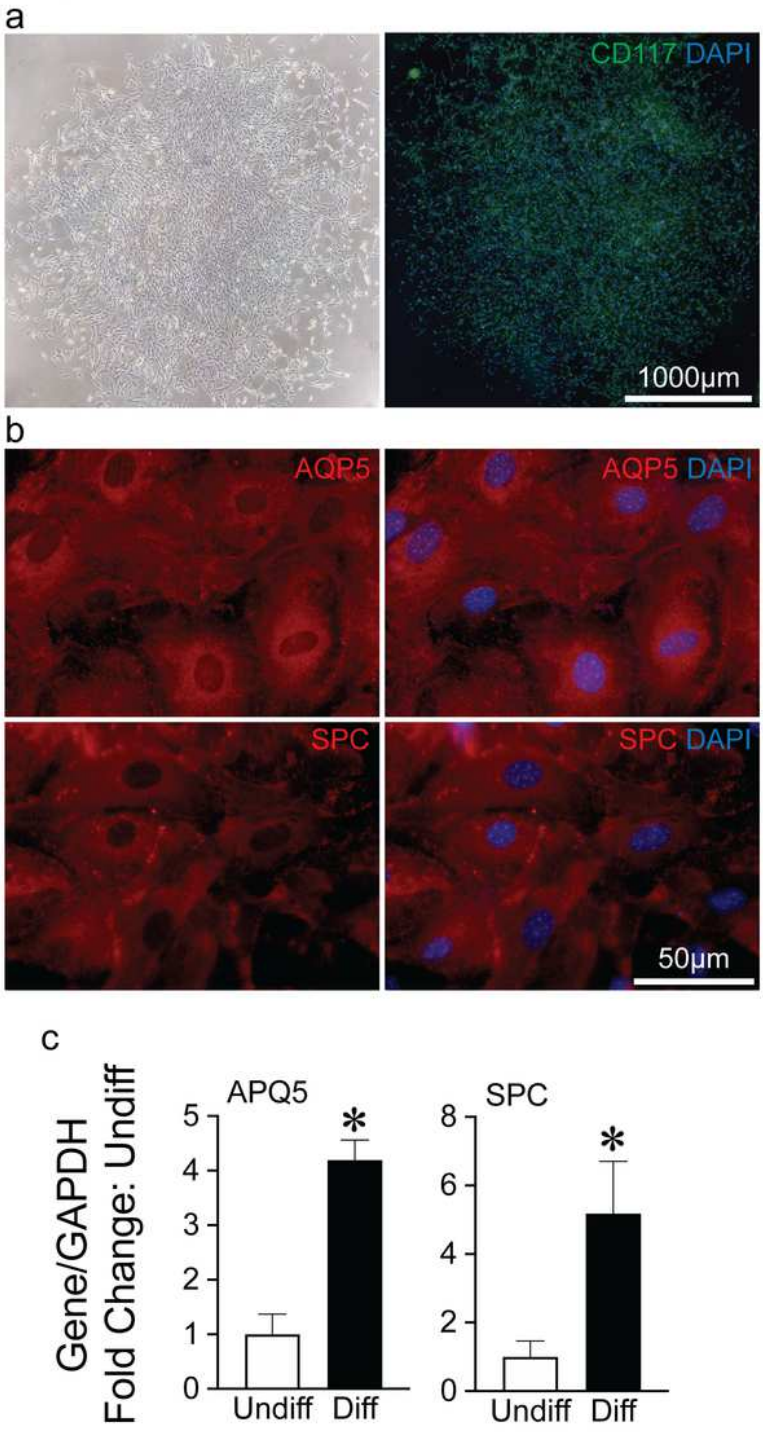

Figure 5

TSCs possess the capability of clone formation and differentiation into alveolar epithelial cells in vitro. TSCs were cultured in a 100-mm dish at limited dilution of one cell every 60 mm2 for 14 days. a) Representative phase contrast images of an entire clone (left), and a clone immunofluorescence stained for CD117 (green, right). DAPI 42 demonstrates nuclear staining (blue). b) TSCs were cultured in epithelial cell differentiation medium on an air liquid interface for 16~18 days. Representative images of these

differentiated cells immunofluorescence stained for AQP5 (red, upper row) and SPC (red, lower row), with merged images including nuclear staining for DAPI (blue, right upper and lower). c) Bar graph showing quantitation of qRT-PCR for AQP5 (right panel) and SPC (left panel) in fold change comparing differentiated (Diff, black bars) to undifferentiated cells (Undiff, white bars), * versus undifferentiated group, P<0.001 for AQP5, P<0.05 for SPC, n=5 for each group.

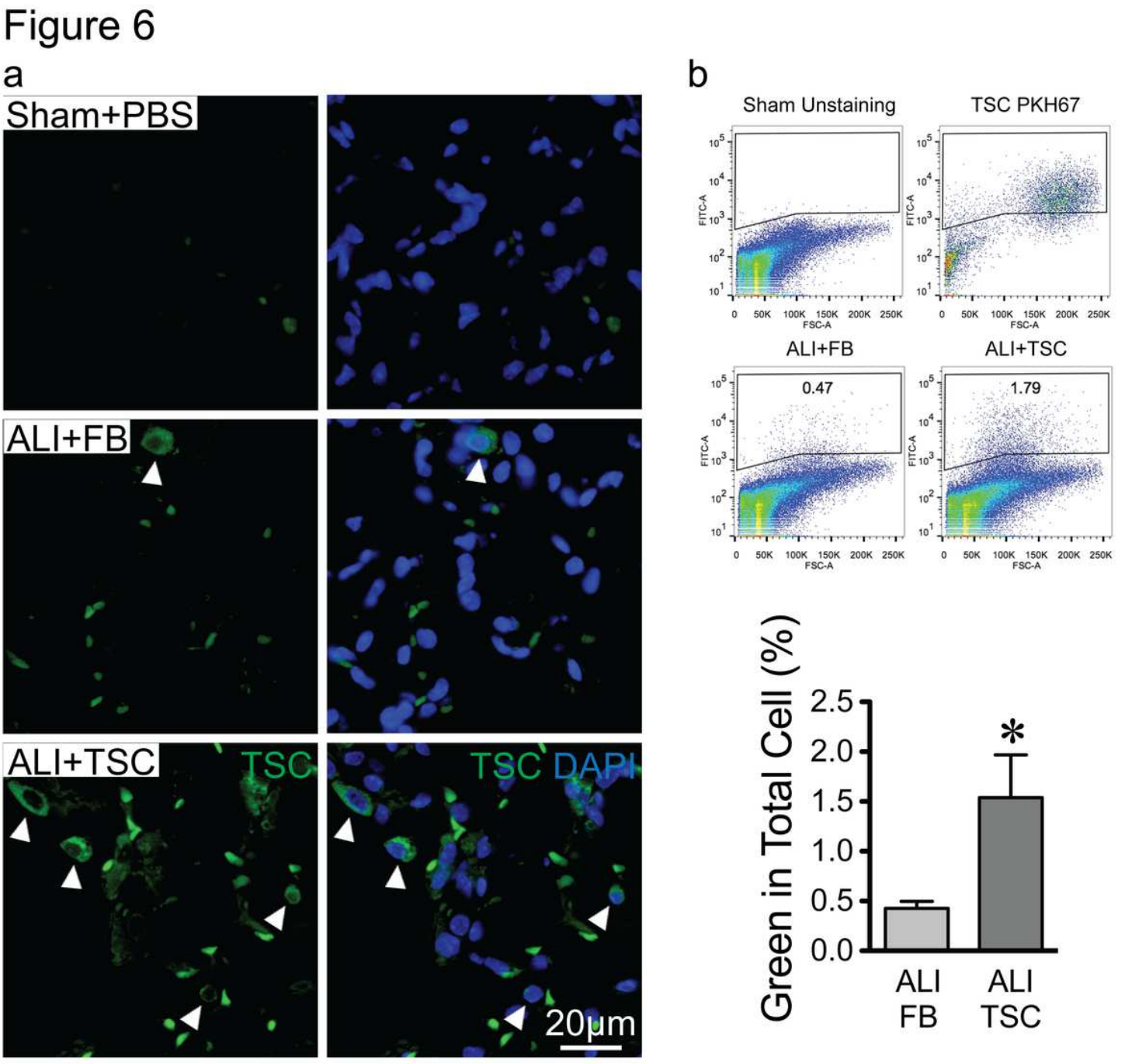

Figure 6

TSCs engraft in the lung injured by BLM. Male 8~10 weeks C57BL/6 mice received PBS (sham) or BLM (ALI) intratracheally. At day 3 after BLM exposure, PBS, FBs, or TSCs were administrated intratracheally. The TSCs and FBs were dyed with PKH67 (green) prior to injection. The lungs were harvested at day 7

after BLM exposure. a) Representative images of the lung, from sham mice (sham+PBS, top row), ALI mice that received FB (ALI+FB, middle row) and TSCs (ALI+TSC, bottom row). Images showing FITC+ cells (green, left column), and merged with nuclear staining for DAPI (blue, right column). White arrowheads point to engrafted cells (green). b) Representative scatter plots of flow cytometry showing the gating strategy: FITC negative (upper left) and PKH67 positive (upper right), FITC+ cells from the lungs of ALI mice that received FBs 43 (ALI+FB, lower left) and TSCs (ALI+TSC, lower right). Bar graph represents quantitation of % green cells in the total lung suspension. *P<0.05, versus ALI+FB group. n=6 for ALI+FB and n=5 for ALI+TSC.

Figure 7

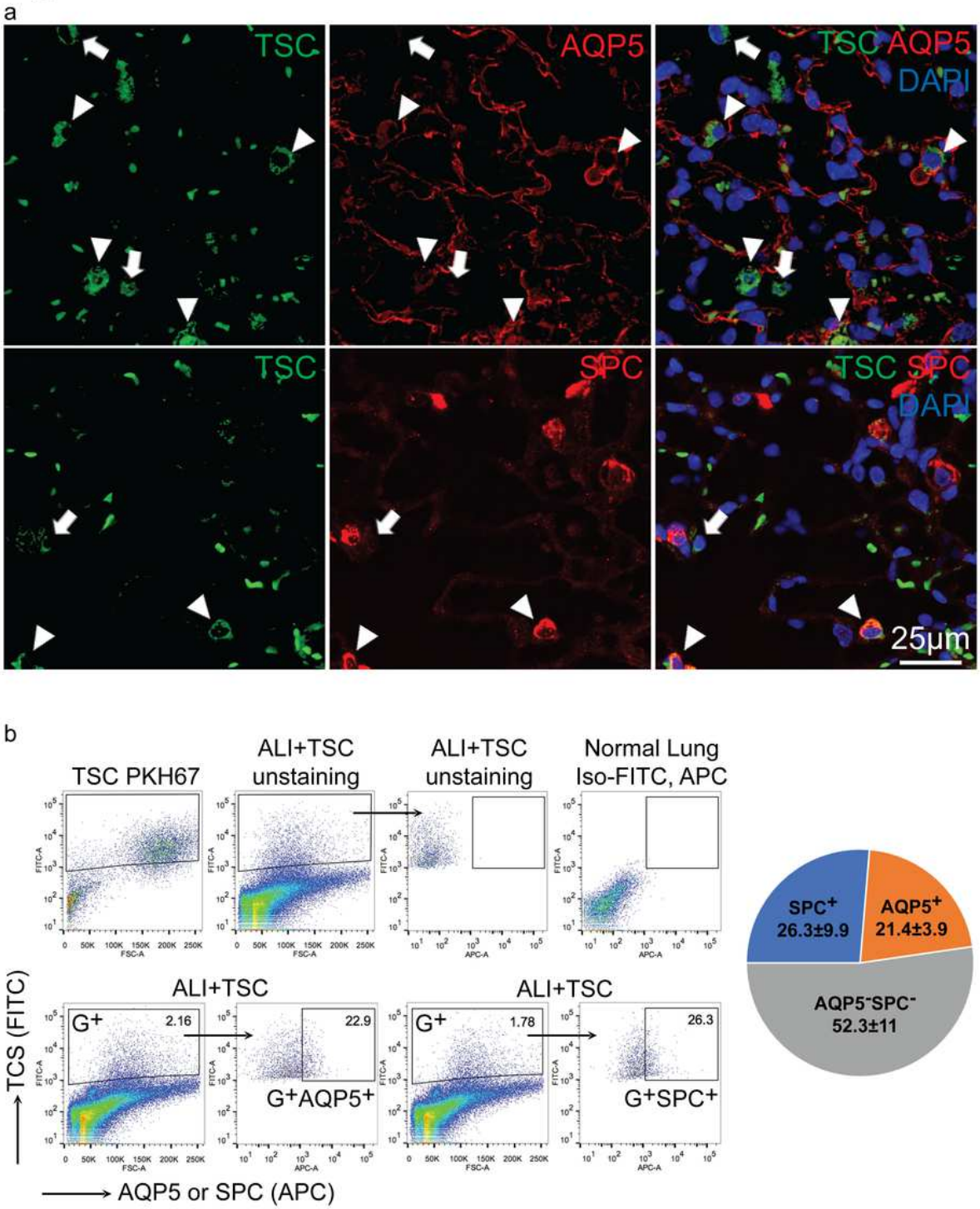

Figure 7

TSCs differentiate into alveolar epithelial cells in the lung injured by BLM. TSCs were pre-labeled with PKH67 (green) and then intratracheally injected into the lungs at day 3 after BLM exposure. The lungs were harvested at day 7 for histologic assessment. a) Representative images of the lung immunofluorescence staining for AQP5 and SPC (red, middle column), TSC pre-labeled with PKH67 (green, left column), and merged images with nuclear staining for DAPI (blue, right column). White

arrowheads point to green+APQ5+ and green+SPC+ cells (upper and lower rows, respectively). White arrows point to green+AQP5–and green+SPC– cells (upper and lower rows, respectively). b) Representative scatter plots of flow cytometry showing the gating strategy (upper row), FITC+ control from TSCs stained with PKH67 (first panel), FITC+ TSCs gated from unstained cells of the lung that received PKH67-prelabeled TSCs (second panel), APC+ gated from the population of FITC+ cells in the second panel (third panel), and isotype control from the normal lung stained with FITC- and APC-isotypes (fourth panel). The lower row shows representative scatter plots of flow cytometry. The cells from BLM injured lungs receiving pre-labeled TSCs (FITC) and were stained for APQ5 44 or SPC (APC). The percentage of FITC+ cells in the total lung cell population is shown in the gates (G+, lower row, the first and third panels), in which these cells gated for a percentage of FITC+AQP5+ and FITC+SPC+ in total FITC+ 3 cells (second and fourth panels, respectively). The pie graph shows quantitation of FITC+APQ5+ and FITC+SPC+ in the total FITC+ cells. n=5 for each group.

Supplementary Files

This is a list of supplementary files associated with this preprint. Click to download.

- Additionalfile2.pdf
- Additionalfile1.pdf